doi:10.1038/nature10489

Active tactile exploration using a brain–machine–brain interface

Joseph E. O'Doherty[1,2], Mikhail A. Lebedev[2,3], Peter J. Ifft[1,2], Katie Z. Zhuang[1,2], Solaiman Shokur[4], Hannes Bleuler[4] & Miguel A. L. Nicolelis[1,2,3,5,6]

Brain–machine interfaces[1,2] use neuronal activity recorded from the brain to establish direct communication with external actuators, such as prosthetic arms. It is hoped that brain–machine interfaces can be used to restore the normal sensorimotor functions of the limbs, but so far they have lacked tactile sensation. Here we report the operation of a brain–machine–brain interface (BMBI) that both controls the exploratory reaching movements of an actuator and allows signalling of artificial tactile feedback through intracortical microstimulation (ICMS) of the primary somatosensory cortex. Monkeys performed an active exploration task in which an actuator (a computer cursor or a virtual-reality arm) was moved using a BMBI that derived motor commands from neuronal ensemble activity recorded in the primary motor cortex. ICMS feedback occurred whenever the actuator touched virtual objects. Temporal patterns of ICMS encoded the artificial tactile properties of each object. Neuronal recordings and ICMS epochs were temporally multiplexed to avoid interference. Two monkeys operated this BMBI to search for and distinguish one of three visually identical objects, using the virtual-reality arm to identify the unique artificial texture associated with each. These results suggest that clinical motor neuroprostheses might benefit from the addition of ICMS feedback to generate artificial somatic perceptions associated with mechanical, robotic or even virtual prostheses.

Brain–machine interfaces (BMIs) have evolved from 1-d.f. systems[3] to many-d.f. robotic arms[4] and muscle stimulators[5] that perform complex limb movements, such as reaching[6–8] and grasping[9]. However, somatosensory feedback, which is essential for dexterous control[10–12], remains underdeveloped in BMIs. With the exception of a few studies combining BMIs with tactile stimuli applied to the body[13], existing systems rely almost exclusively on visual feedback. Prosthetic sensation has been studied in the context of sensory substitution[14] and targeted reinnervation[15]; however, these approaches have limited application range and channel capacity. To provide a proof-of-concept method of equipping neuroprostheses with sensory capabilities, we implemented a BMBI that extracts movement commands from the motor areas of the brain while delivering ICMS feedback in somatosensory areas[1,2,16] to evoke discriminable percepts[17–20]. This idea received support from our pilot study[16], in which a monkey responded to ICMS cues with the movements of a BMI-controlled cursor. However, the ICMS cue did not provide feedback of object–actuator interactions in this previous demonstration.

The BMBI developed here allowed active tactile exploration[21] during BMI control (Fig. 1a). Two monkeys (M and N) received multielectrode implants in the primary motor cortex (M1) and the primary somatosensory cortex (S1) (Fig. 1b). They explored virtual objects using either a computer cursor or a virtual image (avatar) of an arm (Supplementary Fig. 1a, b). In 'hand control', the monkeys moved a joystick with their left hands to position the actuator. They searched through a set of virtual objects, selected one with a particular artificial texture conveyed by ICMS, and held the actuator over that object to obtain reward (Fig. 1a and Supplementary Fig. 1c, d). During 'brain control', the joystick was disconnected and the actuator was controlled by the activity of right-hemisphere M1 neurons[9,22,23]. The behavioural tasks varied in the number of objects on the screen, the artificial textures used and the actuator type (Fig. 2a), and were more difficult than previously reported BMI tasks because of the presence of multiple objects in the workspace, a prolonged object selection period and the necessity of interpreting ICMS feedback.

ICMS was delivered through two pairs of microwires to the hand representation area of S1 in monkey M (Fig. 1c) and through one pair

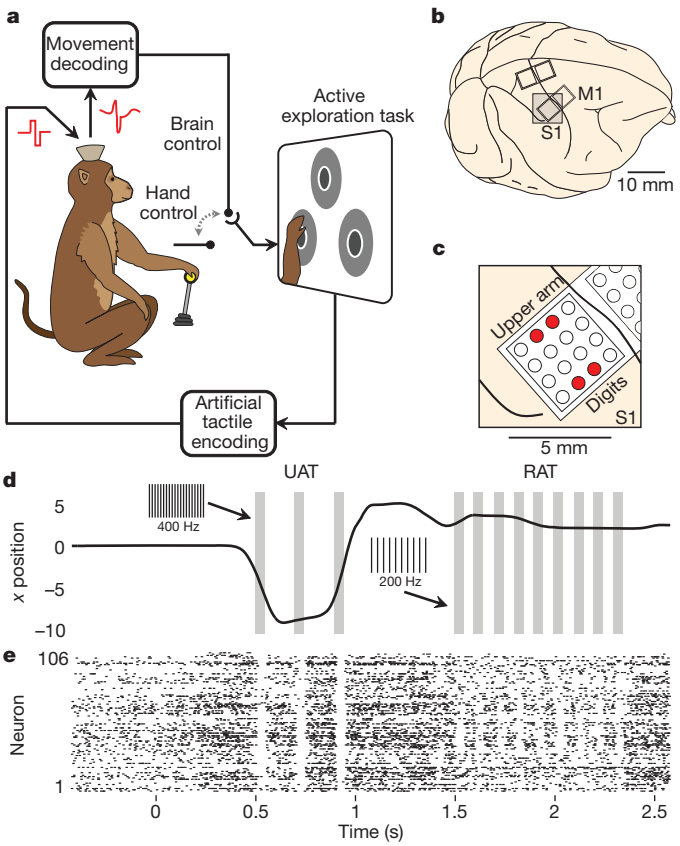

Figure 1 | The brain–machine–brain interface. **a**, Movement intentions are decoded from M1; artificial tactile feedback is delivered to S1. **b**, Microwires were implanted in M1 and S1. **c**, Microwires used for ICMS in monkey M are accented in red. **d**, Actuator movements for a trial in which monkey M explores UAT but ultimately selects RAT. Grey bars indicate stimulation patterns; insets indicate the ICMS frequency. **e**, Rastergram of M1 neurons recorded during the trial shown in **d**.

[1]Department of Biomedical Engineering, Duke University, Durham, North Carolina 27708, USA. [2]Center for Neuroengineering, Duke University, Durham, North Carolina 27710, USA. [3]Department of Neurobiology, Duke University, Durham, North Carolina 27710, USA. [4]STI IMT, École Polytechnique Fédérale de Lausanne, Lausanne CH1015, Switzerland. [5]Department of Psychology and Neuroscience, Duke University, Durham, North Carolina 27708, USA. [6]Edmond and Lily Safra International Institute of Neuroscience of Natal, Natal 59066-060, Brazil.

©2011 Macmillan Publishers Limited. All rights reserved

of microwires to the leg representation in monkey N. Each artificial texture consisted of a high-frequency pulse train presented in packets at a lower, secondary, frequency (Fig. 1d and Supplementary Fig. 2a). The rewarded artificial texture (RAT) consisted of 200-Hz pulse trains delivered in 10-Hz packets. The comparison artificial textures comprised 400-Hz pulse trains delivered in 5-Hz packets (unrewarded artificial texture (UAT)) or an absence of ICMS (null artificial texture (NAT)).

The main challenge solved here was the real-time coupling of ICMS feedback to the BMI decoder. Because ICMS artefacts masked neuronal activity for 5–10 ms after each pulse (Fig. 1d, e), we multiplexed neuronal recordings and ICMS with a 20-Hz clock rate (Supplementary Fig. 2a). The interleaved intervals proved adequate for online motor control and artificial sensation—a result that was not clear a priori because S1 stimulation could have affected M1 processing through the connections between these areas.

BMBI performance improved with training. In task I (Fig. 2a), monkey M surpassed chance performance after nine sessions and monkey N did so after four sessions ($P < 0.001$, one-sided binomial test). Improvement continued with more difficult tasks (tasks II–V) (Fig. 2a, b and Supplementary Fig. 3a). In particular, the time spent exploring unrewarded artificial textures decreased (Fig. 2c and Supplementary Fig. 3b). Additionally, performance improved over the course of daily experimental sessions (Fig. 2d). Psychometric analysis of RAT stimulation amplitudes (Supplementary Fig. 2b) indicated that at least 8 nC per ICMS waveform phase (100-μs-wide current pulses of 80 μA) was needed for the discrimination of artificial textures ($P < 0.001$, one-sided binomial test). Performance was at chance level for catch trials (task II), where ICMS was not delivered ($P = 0.90$, one-sided binomial test).

The statistics of object exploration intervals (total time spent over a particular object in a given trial) indicated that the monkeys uniquely discriminated each type of artificial texture (Figs 2c and 3a, c) and interpreted ICMS within hundreds of milliseconds—a timescale comparable to that for the discrimination of peripheral tactile stimuli[24,25]. Early in task I, exploration intervals were equal for RAT and NAT ($P > 0.5$, Wilcoxon signed-rank test); with training, they became longer for RAT and shorter for NAT (tasks I and II) and UAT (tasks III–V). During hand control, the mean interval was longest for RAT (monkey M: 1,396 ± 21 ms; monkey N: 1,165 ± 15 ms; mean ± s.e.m.), shortest for NAT (304 ± 8 ms; 300 ± 10 ms) and intermediate for UAT (452 ± 13 ms; 402 ± 14 ms) ($P < 0.01$, analysis of variance). During brain control, intervals spent exploring NAT (498 ± 15 ms; 587 ± 25 ms) and UAT (685 ± 20 ms; 764 ± 32 ms) were longer than they were during hand control, but were still shorter than those spent exploring RAT (1,420 ± 28 ms; 1,398 ± 55 ms) ($P < 0.01$, analysis of variance).

Additional hallmarks of active exploration were seen in the conditional probabilities of selecting different artificial textures (Fig. 3b, d). During hand control trials, the monkeys stayed over the first-encountered artificial texture (arrows that loop back to the same

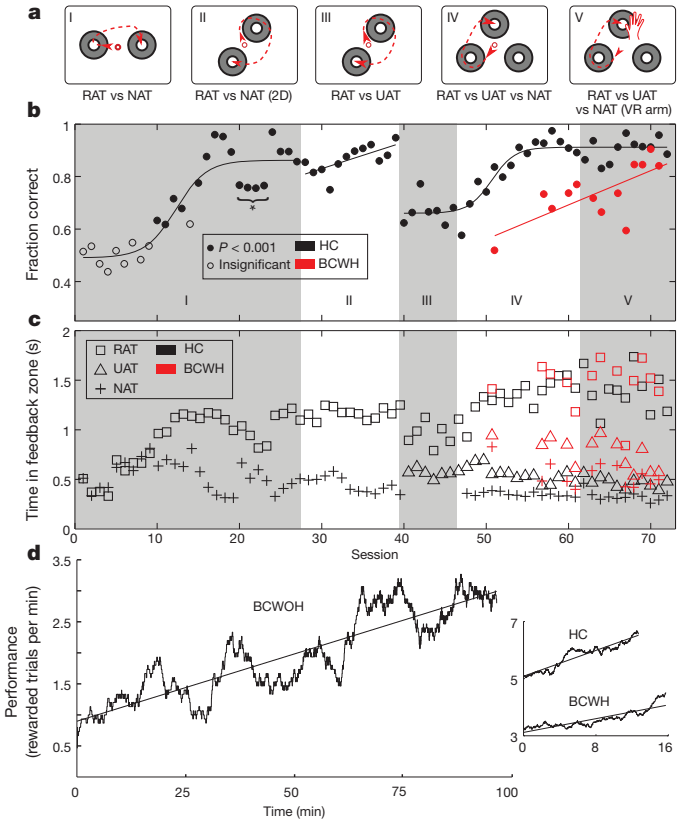

Figure 2 | Learning to use ICMS feedback. **a**, Behavioural tasks. 2D, two-dimensional; VR, virtual reality. **b**, **c**, Performance of monkey M (72 sessions). Circles (**b**) depict the fraction of correctly performed trials. Open circles indicate chance performance. Curves are lines of best fit. The asterisk indicates sessions used for psychometric measurements. Squares, triangles and crosses (**c**) represent mean times spent in RAT, UAT and NAT, respectively. Black, hand control; red, brain control. **d**, Intrasession performance for monkey M. Curves represent averages for brain control without hand movements (BCWOH; main panel, three sessions), for hand control (inset, 12 sessions) and for brain control with hand movements (BCWH; inset, 12 sessions). Lines are best linear fits.

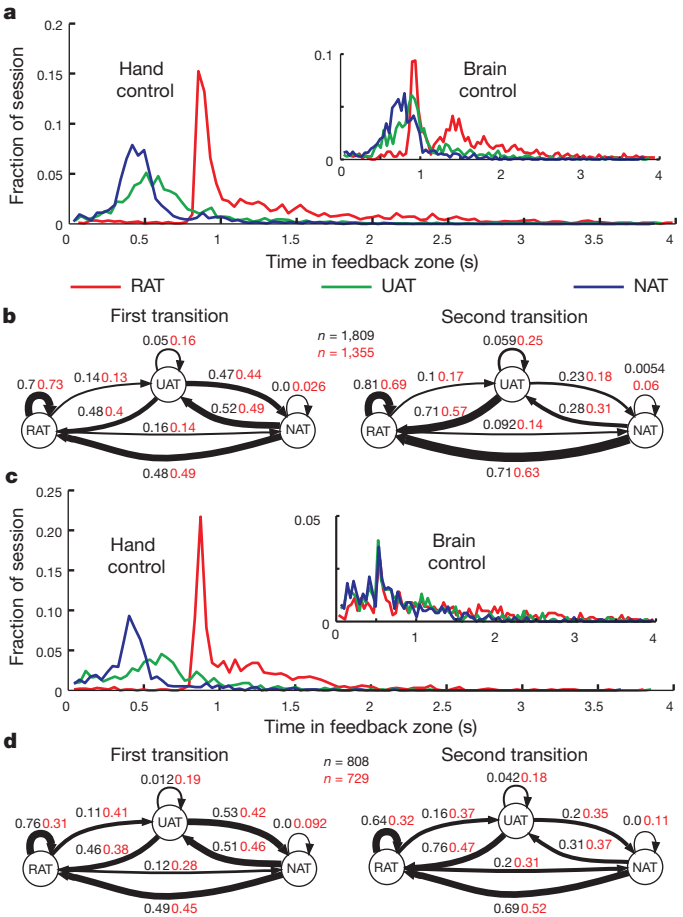

Figure 3 | Statistics of object exploration. **a**, Object exploration intervals during hand control and brain control (inset) for monkey M (hand control: $n = 1{,}809$ trials; brain control: $n = 1{,}355$ trials). **b**, State transition diagrams for monkey M, indicating the probabilities of reaching among RAT, UAT and NAT after the first (left subpanel) or second (right subpanel) reach. Black labels, hand control; red labels, brain control; line thickness is proportional to transition probability. **c**, Same as **a**, but for monkey N (hand control: $n = 808$ trials; brain control: $n = 729$ trials). **d**, Same as **b**, but for monkey N.

©2011 Macmillan Publishers Limited. All rights reserved

artificial texture in Fig. 3b, d) with high probability if it was RAT (monkey M: $P = 0.70$; monkey N: $P = 0.76$), but with low probability if it was UAT ($P = 0.05$; $P = 0.01$) or NAT ($P = 0.0$; $P = 0.0$) (Fig. 3b, d, left). After examining the second artificial texture, the monkeys could identify the correct artificial texture either by apprehending it directly or through a process of elimination. This follows from the increase from chance to approximately $P = 0.7$ in the probability of moving to RAT from NAT or UAT and the decrease to $P \approx 0.2$ in the probability of revisiting UAT or NAT (Fig. 3b, d, right). Similar effects were observed for brain control (Fig. 3b, d, red text).

Brain control started in task IV. During BCWH, the monkeys continued to hold the joystick although it was disconnected[16,22]. During BCWOH[9,22], the joystick was removed. In monkey M, with more than 200 recorded neurons, performance was less accurate during BCWH (73.75 ± 3.00%; mean ± s.e.m.) than during hand control (91.48 ± 1.20%). In monkey N, with 50 recorded neurons, performance dropped further (50.37 ± 3.74% versus 91.45 ± 1.91%), but still significantly exceeded the 33% chance level. M1 neurons showed directionally tuned modulations (Supplementary Figs 5 and 6) that were retained across different interfering ICMS patterns during both hand control (Supplementary Fig. 4a, b) and brain control (Fig. 4a, b).

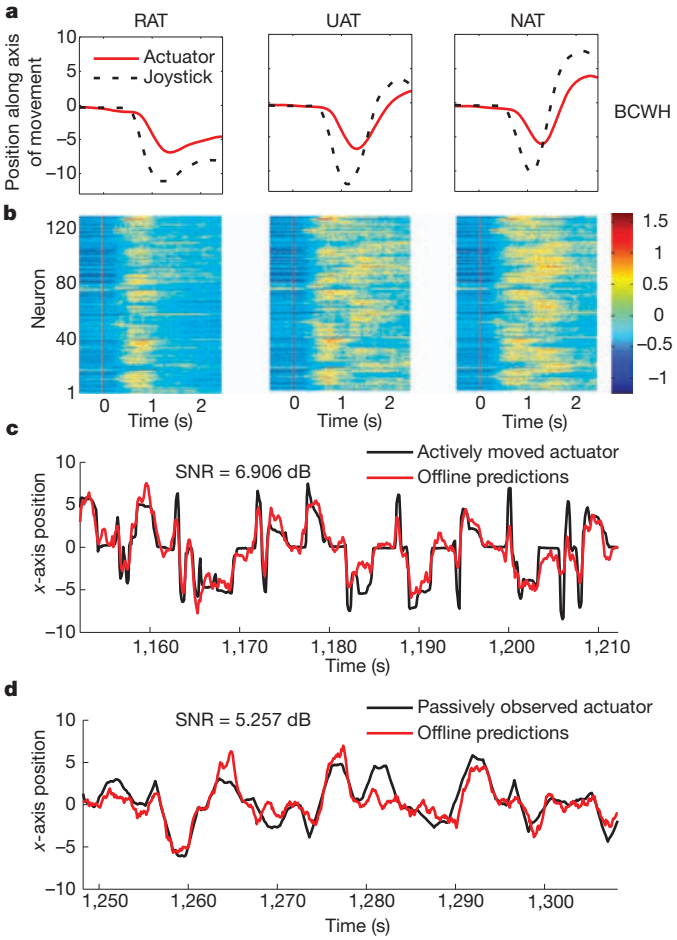

Figure 4 | M1 modulations during active control versus passive observation. **a**, **b**, Average brain control movements for monkey M ($n = 294$ trials) towards the RAT, UAT and NAT objects appearing on the left-hand side of the screen (**a**), and corresponding neuronal modulations (**b**). The colour scale shows normalized firing rate (Hz). Only trials with subsequent anticlockwise reaching movements are included in the middle and right subpanels. Red vertical lines indicate object onset. Firing rate normalized by s.d. **c**, **d**, Position of the actuator actively controlled (**c**) and passively observed (**d**) by monkey M. SNR, signal-to-noise ratio.

In BCWOH, task requirements were eased: the object selection period was reduced to 300–500 ms and monkeys were allowed to overstay at an incorrect object. The performance of monkey M, measured as the number of rewards per minute, steadily improved from 1.021 ± 0.007 to 2.962 ± 0.005 (mean ± s.e.m.; Fig. 2d). Similar improvements were observed for hand control and BCWH (Fig. 2d, inset). The average frequency of actuator displacements, calculated from power spectra, was correlated with the improvement in performance during BCWOH ($R^2 = 0.16$ for the horizontal (x) coordinate and $R^2 = 0.26$ for the vertical (y) coordinate; $P < 0.001$, F-test), which indicated that the monkey modulated its brain activity to scan the targets faster. This behaviour was not random, as the exploration interval for NAT (3,620 ± 350 ms; mean ± s.e.m.) was significantly shorter ($P < 0.02$, Wilcoxon rank-sum test) than for UAT (4,270 ± 310 ms). The exploration of RAT (2,255 ± 94 ms) was the shortest owing to the reduced selection period. For monkey N, BCWOH performance (2.084 ± 0.085 rewards per minute) did not change within sessions, and the differences in exploration intervals were not significant.

In agreement with others[26–30], we observed that M1 neurons represented the movements of the actuator even when it was passively observed by the monkey (Supplementary Fig. 7). Actuator movements (task V) replayed for the monkeys could be reconstructed from M1 activity, using a separately trained decoder (Fig. 4d), with accuracy similar to that in reconstructions made for hand control (Fig. 4c). M1 representation of the passively viewed actuator is consistent with our suggestion that a neuroprosthetic limb might become incorporated in brain circuitry[1].

Our BMBI demonstrated direct bidirectional communication between a primate brain and an external actuator. Because both the afferent and efferent channels bypassed the subject's body, we propose that BMBIs can effectively liberate a brain from the physical constraints of the body. Accordingly, future BMBIs may not be limited to limb prostheses but may include devices designed for reciprocal communication among neural structures and with a variety of external actuators.

METHODS SUMMARY

All animal procedures were performed in accordance with the National Research Council's Guide for the Care and Use of Laboratory Animals and were approved by the Duke University Institutional Animal Care and Use Committee. Two rhesus monkeys were implanted with microwire arrays in both brain hemispheres. These implants were used for both recordings and ICMS (symmetric, biphasic, charge-balanced pulse trains; 100–200 μs, 120–200 μA). Monkeys manipulated a joystick to cause an actuator (computer cursor or a virtual-reality arm) to reach towards up to three objects displayed on a computer monitor. The task required searching for the single object with particular artificial tactile properties. Objects consisted of a central response zone and a peripheral feedback zone. Artificial tactile feedback was delivered when the actuator entered the feedback zone and continued in the response zone. Holding the actuator over the correct object for 0.8–1.3 s produced a reward (fruit juice). Holding the actuator over an incorrect object cancelled the trial. In brain control trials, the actuator was controlled by cortical ensemble activity decoded using an unscented Kalman filter[23]. An interleaved scheme of alternating recording and stimulation subintervals (50 ms each, 50% duty cycle) was implemented to achieve concurrent afferent and efferent operations. In all offline analyses, ICMS periods were excluded from calculations of neuronal firing rates. The virtual-reality arm was animated using MOTIONBUILDER (Autodesk).

Full Methods and any associated references are available in the online version of the paper at www.nature.com/nature.

Received 2 June; accepted 17 August 2011.
Published online 5 October 2011.

1. Lebedev, M. A. & Nicolelis, M. A. Brain-machine interfaces: past, present and future. *Trends Neurosci.* **29,** 536–546 (2006).
2. Nicolelis, M. A. & Lebedev, M. A. Principles of neural ensemble physiology underlying the operation of brain-machine interfaces. *Nature Rev. Neurosci.* **10,** 530–540 (2009).

©2011 Macmillan Publishers Limited. All rights reserved

3. Chapin, J. K., Moxon, K. A., Markowitz, R. S. & Nicolelis, M. A. L. Real-time control of a robot arm using simultaneously recorded neurons in the motor cortex. *Nature Neurosci.* **2,** 664–670 (1999).
4. Velliste, M., Perel, S., Spalding, M. C., Whitford, A. S. & Schwartz, A. B. Cortical control of a prosthetic arm for self-feeding. *Nature* **453,** 1098–1101 (2008).
5. Moritz, C. T., Perlmutter, S. I. & Fetz, E. E. Direct control of paralysed muscles by cortical neurons. *Nature* **456,** 639–642 (2008).
6. Wessberg, J. *et al.* Real-time prediction of hand trajectory by ensembles of cortical neurons in primates. *Nature* **408,** 361–365 (2000).
7. Taylor, D. M., Helms-Tillery, S. I. & Schwartz, A. B. Direct cortical control of 3D neuroprosthetic devices. *Science* **296,** 1829–1832 (2002).
8. Serruya, M. D., Hatsopoulos, N. G., Paninski, L., Fellows, M. R. & Donoghue, J. P. Instant neural control of a movement signal. *Nature* **416,** 141–142 (2002).
9. Carmena, J. M. *et al.* Learning to control a brain-machine interface for reaching and grasping by primates. *PLoS Biol.* **1,** e42 (2003).
10. Johansson, R. S. & Westling, G. Roles of glabrous skin receptors and sensorimotor memory in automatic control of precision grip when lifting rougher or more slippery objects. *Exp. Brain Res.* **56,** 550–564 (1984).
11. Flanagan, J. R. & Wing, A. M. Modulation of grip force with load force during point-to-point arm movements. *Exp. Brain Res.* **95,** 131–143 (1993).
12. James, T. W., Kim, S. & Fisher, J. S. The neural basis of haptic object processing. *Can. J. Exp. Psychol.* **61,** 219–229 (2007).
13. Chatterjee, A. Aggarwal, V. Ramos, A., Acharya, S. & Thakor, N. V. A brain-computer interface with vibrotactile biofeedback for haptic information. *J. Neuroeng. Rehabil.* **4,** 40 (2007).
14. Kaczmarek, K., Webster, J., Bach-y-Rita, P. & Tompkins, W. Electrotactile and vibrotactile displays for sensory substitution systems. *IEEE Trans. Biomed. Eng.* **38,** 1–16 (1991).
15. Marasco, P. D., Schultz, A. E. & Kuiken, T. A. Sensory capacity of reinnervated skin after redirection of amputated upper limb nerves to the chest. *Brain* **132,** 1441–1448 (2009).
16. O'Doherty, J. E., Lebedev, M. A., Hanson, T. L., Fitzsimmons, N. A. & Nicolelis, M. A. A brain-machine interface instructed by direct intracortical microstimulation. *Front. Integr. Neurosci.* **3,** 20 (2009).
17. Richer, F., Martinez, M., Robert, M., Bouvier, G. & Saint-Hilaire, J. M. Stimulation of human somatosensory cortex: tactile and body displacement perceptions in medial regions. *Exp. Brain Res.* **93,** 173–176 (1993).
18. London, B. M., Jordan, L. R., Jackson, C. R. & Miller, L. E. Electrical stimulation of the proprioceptive cortex (area 3a) used to instruct a behaving monkey. *IEEE Trans. Neural Syst. Rehabil. Eng.* **16,** 32–36 (2008).
19. Romo, R., Hernandez, A., Zainos, A. & Salinas, E. Somatosensory discrimination based on cortical microstimulation. *Nature* **392,** 387–390 (1998).
20. Fitzsimmons, N. A., Drake, W., Hanson, T. L., Lebedev, M. A. & Nicolelis, M. A. Primate reaching cued by multichannel spatiotemporal cortical microstimulation. *J. Neurosci.* **27,** 5593–5602 (2007).
21. Lederman, S. J. & Klatzky, R. L. Hand movements: a window into haptic object recognition. *Cognit. Psychol.* **19,** 342–368 (1987).
22. Lebedev, M. A. *et al.* Cortical ensemble adaptation to represent velocity of an artificial actuator controlled by a brain-machine interface. *J. Neurosci.* **25,** 4681–4693 (2005).
23. Li, Z. *et al.* Unscented Kalman filter for brain-machine interfaces. *PLoS ONE* **4,** e6243 (2009).
24. Lebedev, M. A., Denton, J. M. & Nelson, R. J. Vibration-entrained and premovement activity in monkey primary somatosensory cortex. *J. Neurophysiol.* **72,** 1654–1673 (1994).
25. Liu, Y., Denton, J. M. & Nelson, R. J. Neuronal activity in primary motor cortex differs when monkeys perform somatosensory and visually guided wrist movements. *Exp. Brain Res.* **167,** 571–586 (2005).
26. Cisek, P. & Kalaska, J. F. Neural correlates of mental rehearsal in dorsal premotor cortex. *Nature* **431,** 993–996 (2004).
27. Graziano, M. S., Cooke, D. F. & Taylor, C. S. Coding the location of the arm by sight. *Science* **290,** 1782–1786 (2000).
28. Maravita, A. & Iriki, A. Tools for the body (schema). *Trends Cogn. Sci.* **8,** 79–86 (2004).
29. Tkach, D., Reimer, J. & Hatsopoulos, N. G. Observation-based learning for brain-machine interfaces. *Curr. Opin. Neurobiol.* **18,** 589–594 (2008).
30. Dushanova, J. & Donoghue, J. Neurons in primary motor cortex engaged during action observation. *Eur. J. Neurosci.* **31,** 386–398 (2010).

Supplementary Information is linked to the online version of the paper at www.nature.com/nature.

Acknowledgements We thank D. Dimitrov for conducting the animal neurosurgeries; G. Lehew and J. Meloy for building brain implants; J. Fruh for rendering the virtual-reality monkey arm; T. Phillips, L. Oliveira and S. Halkiotis for technical support; and E. Thomson and Z. Li for comments. This research was supported by DARPA (award N66001-06-C-2019), TATRC (award W81XWH-08-2-0119), the NIH (award NS073125), NICHD/OD (award RC1HD063390) and NIH Director's Pioneer Award DP1OD006798, to M.A.L.N. The content is solely the responsibility of the authors and does not necessarily represent the official views of the Office of the NIH Director or the NIH.

Author Contributions J.E.O'D., M.A.L. and M.A.L.N. designed experiments, analysed data and wrote the paper; J.E.O'D., M.A.L., P.J.I. and K.Z.Z. conducted experiments; and S.S. and H.B. developed the virtual-reality monkey arm.

Author Information Reprints and permissions information is available at www.nature.com/reprints. The authors declare no competing financial interests. Readers are welcome to comment on the online version of this article at www.nature.com/nature. Correspondence and requests for materials should be addressed to M.A.L.N. (nicoleli@neuro.duke.edu).

©2011 Macmillan Publishers Limited. All rights reserved

METHODS

Subjects and implants. Two adult rhesus macaque monkeys (*Macaca mulatta*) participated in this study. Each monkey was implanted with four 96-microwire arrays constructed of stainless steel 304. Each hemisphere received two arrays: one in the upper-limb representation area and one in the lower-limb representation area. These arrays sampled neurons in both M1 and S1. We used recordings from the right-hemisphere arm arrays in each monkey, because each manipulated the joystick with its left hand. Within each array, microwires were grouped in two four-by-four, uniformly spaced grids each consisting of 16 electrode triplets. The separation between electrode triplets was 1 mm. The electrodes in each triplet had three different lengths, increasing in 300-μm steps. The penetration depth of each triplet was adjusted with a miniature screw. After adjustments during the month following the implantation surgery, the depth of the triplets was fixed. The longest electrode in each triplet penetrated to a depth of 2 mm as measured from the cortical surface.

Tasks. The monkeys were trained to manipulate a computer cursor or a virtual-reality arm and to reach, using this actuator, towards objects displayed on a computer monitor. The objects were visually identical, but had different tactile properties as conveyed by ICMS of S1. In hand control, each trial commenced when the monkey held the joystick with their working hand. Then a target appeared in the centre of the screen. The monkey had to hold the actuator within that centre target for a random hold time uniformly drawn from the interval 0–2 s. After this, the central target disappeared and was replaced by a set of virtual objects radially arranged about the centre of the screen. Each of these consisted of a central response zone and a peripheral feedback zone, distinguished by their shading (Supplementary Fig. 1c). Tactile feedback was delivered in the feedback zone or the corresponding response zone. For monkey M, the radius of the response zone varied from 1.5 to 4.0 cm and the radius of the feedback zone varied from 4.5 to 7.25 cm, across all tasks and sessions. For monkey N, the radius of the response zone varied from 1.5 to 4.5 cm and the radius of the feedback zone varied from 4.75 to 9.5 cm, across all tasks and sessions. A trial was concluded when the monkey placed the actuator within the response zone for a hold interval (800–1,300 ms for hand control, depending on the session; 300–500 ms for brain control) or the monkey released the joystick handle (in hand control trials). The next trial commenced after an intertrial interval of 500 ms.

The sequence of events was the same during brain control trials. In some brain control sessions, the joystick was removed from the behavioural set-up. For these, each new trial commenced following the previous intertrial interval without the requirement for the monkey to hold the joystick. In tasks I–III, monkeys chose from a set of two objects. In task I, the monkeys had to choose between RAT and NAT for fixed object locations. In task II, RAT and NAT were presented on the screen at different angular locations in each trial. In task III, object number and spatial arrangement were the same as in task II, but RAT and UAT were used. In task IV, three objects were used (RAT, UAT and NAT) and their arrangement on the screen varied from trial to trial. Finally, in task V, the virtual-reality monkey arm replaced the computer cursor.

Psychometric measurements. Psychometric measurements determined the minimum ICMS amplitude that the monkeys could discriminate (Supplementary Fig. 2b). In these measurements, the ICMS amplitude was different in every trial. In each psychometric session, a range of amplitudes was selected such that about half were in a range clearly above the monkeys' threshold for discrimination and half were in a range of unknown discriminability.

Catch trials. In some sessions, a small percentage of trials (typically 1%) were designated as catch trials. In these trials, the microstimulator delivered pulse trains with zero amplitude, but all other aspects of the behavioural task remained the same. This allowed us to confirm that there were no unintentional sources of information that the monkeys could use to perform the tasks.

Algorithms. An *N*th-order unscented Kalman filter[23] (UKF) was used for brain control predictions. Up to a tenth-order UKF was used in some sessions, but in most sessions we found that the third-order UKF was sufficient. The filter parameters were fitted on the basis of either the hand movements of the monkeys while they performed the task using a joystick or on passive observation of actuator movements while the monkeys' arms were restrained.

ICMS. Symmetric, biphasic, charge-balanced pulse trains were delivered in a bipolar fashion across pairs of microwires. The channels selected had clear sensory receptive fields in the upper limb (monkey M: two pairs of microwires with synchronous pulse trains) or lower limb (monkey N: one pair of microwires). For monkey M, the anodic and cathodic phases of stimulation had a pulse width of 105 μs; for monkey N, the pulse width was 200 μs. The anodic and cathodic phases of the stimulation waveforms were separated by 25 μs.

Interleaved ICMS and recordings. We implemented an interleaved scheme of alternating recording and stimulation intervals (Supplementary Fig. 2a). Our BMI had a 10-Hz update rate. That is, 100 ms of past neural data were used to make predictions about the desired state of the actuator. We broke up each 100-ms interval into two 50-ms subintervals. In the first subinterval (Rec), neural activity was recorded as usual and the measured spike count was used to estimate the firing rate for the whole 100-ms interval. The second subinterval (Stim) was reserved exclusively for delivering ICMS; all spiking activity occurring in this subinterval was discarded. Whenever the actuator was in contact with a virtual object at the start of a Stim interval, an ICMS pulse train was delivered. For RAT, nine pulses of ICMS were delivered; for UAT, 18 pulses of ICMS were delivered; and for NAT, no pulses of ICMS were delivered. The neural activity in the Stim interval was discarded even for NAT, so that there would be no bias induced by ICMS-occluded neural data.

Virtual-reality monkey arm. In task V, we introduced a novel, brain-controlled virtual-reality arm with realistic kinematic movements and spatial interactions. The control loop rate was 50 Hz, with visual refreshing at 30 Hz. The arm model was designed to depict a rhesus macaque. We presented a first-person perspective of the virtual-reality arm to the monkey, who controlled the position of the hand. Arm posture was controlled using a mixture of direct control of end effectors and inverse kinematics, constrained by the physical interdependencies of the joints.

©2011 Macmillan Publishers Limited. All rights reserved